

Halochromic and antioxidant capacity of smart films of chitosan/chitin nanocrystals with curcuma oil and anthocyanins

Rut Fernández-Marín^{a,**}, Susana C.M. Fernandes^b, M^a Ángeles Andrés Sánchez^a, Jalel Labidi^{a,*}

^a Environmental and Chemical Engineering Department, University of the Basque Country UPV/EHU, Plaza Europa 1, 20018, Donostia-San Sebastián, Spain

^b Université de Pau et des Pays de L'Adour, E2S UPPA, IPREM, CNRS, 64600 Anglet, France

ARTICLE INFO

Keywords:

Curcuma oil
Anthocyanins
Halochromic capacity
Smart pH-sensitive materials
Chitin nanocrystals
Nanocomposite films

ABSTRACT

Curcuma longa L. essential oil and anthocyanin extracts contain bioactive compounds such as antioxidant properties and their pigments are able to change color when exposed to different pH or ammonium gas. In this context, the objective of the present work was to develop pH-sensitive intelligent films by adding curcuma oil (composed of essential oils and pigments) and anthocyanin extracts to a chitosan matrix reinforced with alpha-chitin nanocrystals. The incorporation of curcuma oil, anthocyanins and nanocrystals enhanced the mechanical properties and hydrophobicity; and, decreased water solubility and moisture content. In addition, the films also showed almost total blocking against UV/Vis light at wavelengths below 550 nm. Interestingly, the films were at the same time antioxidant, and sensitive to color change when exposed to ammonia gas and different pH solutions, with greater variations observed when higher concentrations of curcuma oil were added. Hence, these results revealed the potential of these films as intelligent food packaging applications.

1. Introduction

Food packaging has an important role in storage, transport and especially regarding food spoilage delay (Qianyun Ma, Liang, Cao, & Wang, 2018). Thus, it has been observed a growing interest into improving packaging to prevent food deterioration caused by light, moisture, oxygen or the proliferation of microorganisms (S. Chen, Zhang, Bhandari, & Yang, 2020). In this context, lately, smart packaging containing an indicator (thermal, leakage, water or gas permeability indicators) to quickly inform the consumer about the quality status of the food, has generated a great interest in food industry (Alizadeh-Sani, Tavassoli, McClements, & Hamishehkar, 2021; Kalpana, Priyadarshini, Maria Leena, Moses, & Anandharamkrishnan, 2019; Xin Zhang, Zou, et al., 2019). For instance, pH-sensitive films containing colorimetric indicators that changed the color when the food, especially meat and fish, decompose and release basic volatile organic amines (S. Chen, Zhang, et al., 2020; Liang, Sun, Cao, Li, & Wang, 2019; Pereira, de Arruda, & Stefani, 2015; Yong, Wang, Zhang, et al., 2019; Xin Zhang, Zou, et al., 2019).

Natural compounds, which are safe for human health and the environment, biodegradable, non-toxic and with antimicrobial and

antioxidant properties, have been used as alternative to the synthetic indicators. Examples of these natural indicators are pigments extracted from plants such as anthocyanins and curcuma oil extracted from curcuma or turmeric root (*Curcuma longa* L.). Anthocyanins are water-soluble pigments and can be extracted from different sources as purple potato, blackberry, roselle, purple onion peel, red cabbage or black chokeberry among others. They present excellent antimicrobial, antioxidant and pH-sensitive properties (S. Chen, Zhang, et al., 2020; Halász & Csóka, 2018; Li et al., 2019a; Qianyun Ma et al., 2018; Pereira et al., 2015; Wu et al., 2020; Zhai et al., 2017). Curcuma oil has as major compound, curcumin, a yellow pigment that is pH-sensitive (halochromic) due to its enol and keto tautomeric forms (Sahne, Mohammadi, Najafpour, & Moghadamnia, 2017). Moreover, this oil, can be used as a bioactive agent since its properties include antimicrobial and antioxidant properties (Chaaban et al., 2019; Fernández-Marín, Fernandes, Andrés, & Labidi, 2021). Recently, it was also shown that mixing different pigments improves the range of color change as well as antioxidant properties (H. Zhi Chen, Zhang, et al., 2020; Zhu et al., 2021).

Therefore, different matrices including k-carrageenan, starch and chitosan among others have been used in order to immobilise and apply

* Corresponding author.

** Corresponding author.

E-mail addresses: rut.fernandez@ehu.es (R. Fernández-Marín), jalel.labidi@ehu.es (J. Labidi).

<https://doi.org/10.1016/j.foodhyd.2021.107119>

Received 23 May 2021; Received in revised form 13 August 2021; Accepted 15 August 2021

Available online 19 August 2021

0268-005X/© 2021 The Author(s).

Published by Elsevier Ltd.

This is an open access article under the CC BY-NC-ND license

(<http://creativecommons.org/licenses/by-nc-nd/4.0/>).

anthocyanins or/and curcuma oil in food packaging (H. zhi Chen, Zhang, et al., 2020; Koshy et al., 2021; Y. Liu, Wang, et al., 2019; Yong, Wang, Bai, et al., 2019). For instance, H. Zhi Chen et al. investigated the behaviour of mixing curcumin and anthocyanins in a matrix of starch, poly(vinyl alcohol) and glycerol to test the pH change on the freshness of fish (H. Zhi Chen, Zhang, et al., 2020). Among these matrices, chitosan (poly- β -(1-4)-N-acetyl-D-glucosamine, CS), which is obtained from the deacetylation of chitin, has been largely used for food packaging because of its unique properties such as non-toxicity, biocompatibility, biodegradability, excellent film-forming properties (Salaberria, Fernandes, Diaz, & Labidi, 2015; Yong, Wang, Bai, et al., 2019). However, CS films have disadvantages including low UV light barrier and limited mechanical properties. Thus, nanocrystals or nanofibres from cellulose or chitin have been incorporated as reinforcing agents (Claverie, McReynolds, Petitpas, Thomas, & Fernandes, 2020; Fernández-Marín, Labidi, Andrés, & Fernandes, 2020; Joseph et al., 2020; Salaberria, Labidi, et al., 2015; Salari, Sowti Khiabani, Rezaei Mokarram, Ghanbarzadeh, & Samadi Kafil, 2018; Xinhui; Zhang et al., 2021; Veronica; Zubillaga, Alonso-varona, Fernandes, Salaberria, & Palomares, 2020; Verónica; Zubillaga et al., 2018). In particular, chitin nanocrystals (CHNC) have attracted the interest of the scientific community due to their excellent properties such as antimicrobial, small size, low toxicity and biocompatibility (Fernández-Marín, Labidi, et al., 2020; Salaberria, Labidi, et al., 2015; Salaberria, Diaz, Andrés, Fernandes, & Labidi, 2017). In this sense, Wu et al. developed pH-sensitive smart films with red cabbage anthocyanins using a matrix of oxidized chitin nanocrystals and Konjac glucomannan (Wu et al., 2020).

The present work presents the development of smart multifunctional materials based on chitosan/chitin nanocrystals nanocomposite films and curcuma oil and anthocyanins as pH- and volatile ammonia-sensitive agents. The aim was to obtain final materials with halochromic and antioxidant capacity for the monitoring of food packaging.

2. Materials and methods

2.1. Materials

Ethanol (EtOH, analytical standard), methanol (MeOH, HPLC grade), ammonium hydroxide solution (NH₄OH, ACS reagent, 28–30% NH₃ basis), 6-Hydroxy-2, 5, 7, 8-tetramethylchromane-2-carboxylic acid (Trolox) and 2, 2-diphenyl-1-picrylhydrazyl (DPPH) were supplied by Sigma-Aldrich. Scharlau supplied Folin-Ciocalteu reagent and gallic acid monohydrate (C₇H₆O₅H₂O, extra pure). Hydrochloric acid (HCl, 37%), glycerol anhydrous, sodium hydroxide (NaOH, ACS reagent) and acetic acid glacial (CH₃COOH, technical grade) were provided by Panreac AppliChem. Sodium carbonate anhydrous (NaCO, general-purpose grade) was purchased from Fischer.

2.2. Chitin extraction and nanocrystals isolation, and chitosan production

Chitin was extracted from yellow lobster (*Cervimunda johni*) waste supplied by Antarctic Seafood S.A. (Chile) following the previous method used by (Salaberria, Diaz, Labidi, & Fernandes, 2015b). Then, alpha-chitin nanocrystals (α -CHNC) were isolated *in house* by microwave assisted extraction technique (Discover system, CEM, USA) under the conditions of 10 min, 124.75 W and 1 M HCl (Fernández-Marín, Hernández-Ramos et al., 2021). The ratio used was 1:30 w/v (chitin: HCl) (Salaberria et al., 2015b). The suspension was then filtered, washed with distilled water to neutral pH and stored at 4 °C until use. The degree of acetylation (DA) was determined by solid ¹³C NMR was of 90% (Kasaai, 2010). The crystallinity index (CI %) was of 94% obtained by X-Ray Diffraction (XRD) spectra (Philip X'pert Pro Automatic diffractometer, Amsterdam, Netherlands) (Sagheer, Al-Sughayer, Muslim, & Elsabee, 2009). The morphology of the nanocrystals was carried out by AFM and showed rod-like morphology with an average of 314 ± 63 nm

in lengths and 42 ± 11 nm in width as demonstrated in previous work (Fernández-Marín, Hernández-Ramos et al., 2021). Chitosan (CS) was obtained from lobster (*Homarus gammarus*) by the deacetylation of the obtained chitin (CH) following the methodology described by Salaberria et al. (Salaberria, Diaz, Labidi, & Fernandes, 2015a). For this purpose, a ratio of 1:15 w/v (CH:NaOH 60% w/v) was used at 130 °C under nitrogen atmosphere for 4 h. The obtained CS was filtered, washed and dried at 106 °C for 24 h. The degree of N-acetylation was 13.29% obtained by ¹³C NMR.

2.3. Curcuma oil extraction

Curcuma oil was extracted from the root *Curcuma longa* L. by microwave-assisted extraction (Milestone flexiWAVE, Italy) under the conditions of 29.99 min, 160 W and 1:20 w/v (curcuma powder: EtOH) following the method described by (Fernández-Marín, Fernandes, Andrés, & Labidi, 2021). The composition of the curcuma oil was determined by GC/MS. The major compounds were Ar-turmerone (33.78%), turmerone (20.12%) and β -turmerone (20.05%) as previously described by (Fernández-Marín, Fernandes, Andrés, & Labidi, 2021).

2.4. Anthocyanin extraction

Anthocyanin was extracted from red cabbage (*Brassica oleracea* var. *capitata* f. *rubra*) purchased in a market in Gipúzcoa, Spain. The red cabbage was washed with distillate water and dried at 50.00 ± 0.05 °C. It was then ground (Retsch SM 2000; Germany) and sieved (0.5 × 0.5 mm mesh). Extraction was carried out with 25 g of red cabbage powder in 500 mL of acidified ethanol (85:15 v/v, EtOH:HCl (1M)) with stirring at 50 °C in the dark overnight following the protocol described by Li Y. et al. (Li et al., 2019b). Afterwards, it was filtered and rotavaporated at 45 °C to remove the solvent. The obtained extract was stored in the dark at 4 °C. The composition of red cabbage anthocyanins has been well studied in numerous works including (Mizgier et al., 2016; Uranga, Etxabide, Guerrero, & de la Caba, 2018; Wiczowski, Szawara-Nowak, & Topolska, 2013): cyanidin-3-(sinapoyl) (sinapoyl)-diglucoside-5-glucoside followed by cyanidin-3-(p-coumaroyl)-diglucoside-5-glucoside and cyanidin-3-diglucoside-5-glucoside as the major compounds.

2.5. Preparation of nanocomposite films

To prepare the nanocomposite films, CS (1% w/v) was dissolved in a solution of acetic acid (1% v/v) under stirring for 24 h. After, to this solution, glycerol 0.2% v/v (Cs based) was added as plasticiser and mixed at 15 000 rpm using an Ultra-Turrax (Heidolph Silent Crusher M., Germany) for 10 min at 25 °C. Then, the α -CHNC (0.5% w/v) were added and mixed at 15 000 rpm for 10 min. Afterwards, 5 different bioactive nanocomposite film samples were prepared by adding or curcuma oil (C) or anthocyanin extract (A), in addition 3 different mixtures of both extracts (see Table 1). To prepare the bioactive nanocomposite films, two 2 g/L dilutions were prepared by using or curcuma oil or anthocyanin extract in ethanol, and the nanocomposite films were made by adding 1% v/v of C solution or A extract with respect to the CS.

Table 1
Identification and composition of nanocomposite films.

Sample code	α -CHNC (% w/v)	C (% v/v)	A (% v/v)	C:A (% v/v)
CSNC	0.5	–	–	–
CSNC-C	0.5	1	–	–
CSNC-A	0.5	–	1	–
CSNC-C(A:8:1)	0.5	8	1	8:1
CSNC-C(A:1:8)	0.5	1	8	1:8
CSNC-C(A:1:1)	0.5	1	1	1:1

α -CHNC: alpha-chitin nanocrystals; C: curcuma oil; A: anthocyanin extract; % w/v or % v/v based on chitosan.

The 3 mixtures were prepared by using: (i) 8% v/v C and 1% v/v A; (ii) 1% v/v C and 8% v/v A; and (iii) 1% v/v C and 1% v/v A, all concentration with respect to CS. All suspensions were mixed by using an Ultra-Turrax at 15 000 rpm for 10 min and degassed to remove bubbles. The nanocomposite films were prepared by the solvent-casting technique by using 50 mm diameter Petri dishes at 30 °C for 24 h. CS/chitin nanocrystals nanocomposite films without the extracts were prepared as controls. Before the characterization, the samples were stored in a climatic chamber at 25 °C with a relative humidity of 50 ± 5%. The identification and composition of the nanocomposite films are shown in Table 1.

2.6. Characterization of nanocomposite films

2.6.1. General aspect and physicochemical properties of the nanocomposite films

2.6.1.1. Light transmission and opacity. The transmittance of the nanocomposite films was measured with an UV/Vis spectrophotometer (Jasco V-730 UV/VIS spectrophotometer, JASCO, Germany) in the range 750–250 nm. The opacity was determined by measuring the absorbance at 600 nm with the same UV/Vis spectrophotometer (Fernández-Marín, Labidi, et al., 2020). The following equation (1) was used for its determination:

$$\text{Opacity} = \frac{\text{Abs}_{600}}{\text{Th}} \quad (1)$$

where Abs 600 corresponds to the absorbance at 600 nm and Th is the thickness of each film (mm).

2.6.1.2. Thickness and grammage. The thickness of the nanocomposite films was measured with a digital micrometer (Ultra Präzision Messzeuge GmbH, Glattbach, Germany). Thickness values were measured at 6 random points on the films and expressed as average and standard deviation.

The grammage of the films was calculated by the ratio between the weight of the film and the area of the section studied (1.5 × 3 cm²). It was measured in triplicate for each sample. Grammage (g/m²) = weight (g)/area (m²).

2.6.1.3. Water solubility and moisture content. Water solubility (WS) was measured by cutting 1.5 × 3 cm² rectangles from the nanocomposite films, which were dried at 106 °C for 3 h and then weighed. The portions of the films were then immersed in 50 mL of distilled water with stirring for 24 h at room temperature. The undissolved portion was dried at 106 °C for 24 h. After that time, it was weighed (Sabraee, Milani, Ghanbarzadeh, & Hamishehkar, 2017). Water solubility was calculated using equation (2):

$$\text{WS} (\%) = \frac{(W_0 - W_1)}{W_0} \times 100 \quad (2)$$

where W₀ is the weight before immersion in distilled water (g) and W₁ represents the weight of the undissolved film portion after drying (g). The measurement was carried out in triplicate for each sample and the results were given by the mean and standard deviation.

To measure the moisture content (MC) of the films, the samples were cut into rectangular portions (1.5 × 3 cm²), weighed and dried at 106 °C (Memmert UN160 plus Twindisp, Germany) for 24 h (Fernández-Marín, Labidi, et al., 2020). The MC was determined with the following equation (3):

$$\text{MC} (\%) = \frac{(W_0 - W_1)}{W_1} \times 100 \quad (3)$$

where W₀ is the initial weight of the sample (g) and W₁ represents the

weight after 24 h in the oven (g). The MC measurements of the nanocomposite films were carried out in triplicate and the results were given as the means and their standard deviations.

2.6.1.4. Water contact angle. The water contact angle of the nanocomposite films was measured with an Oca20 DataPhysics equipment (DataPhysics Instruments GmbH, Filderstadt, Germany). 5 µL distilled water droplet was deposited on the sample surface and the contact angles on the surface were determined at room temperature at 0 and 2 min using the SCA20 software. For each film 4 replicates were measured.

2.6.2. Mechanical properties and thermogravimetric analysis (TGA)

The mechanical properties of the samples were measured using an Instron 5967 testing equipment (Instron, Norwood, MA, USA). From each sample, eight rectangular samples of 0.5 × 4.5 cm² were cut and the tensile strength (TS), Young's modulus (YM) and elongation (E %) were determined. The load cell used was 500 N and the transverse test rate was 3 mm/min.

TGA analyses were carried out with the Mettler Toledo TGA/SDTA 851 instrument (New Castle, DE, USA). About 5 mg of each sample was used and a heating ramp of 10 °C/min from 25 °C to 750 °C under nitrogen atmosphere was employed.

2.6.3. pH- and volatile ammonia-sensitivity assessment

In order to evaluate the halochromic capacity of the samples, the films were exposure to pH-variations and volatile ammonia as follows:

- **Volatile ammonia:** this experiment was carried out using the method described by (Zhai et al., 2017) with slight modification. First, the films were cut into 2 × 4 cm. Then, each sample was subjected to two different concentrations of ammonia solutions (0.008 mol/L and 0.5 mol/L), by using separately, 70 mL of each ammonium solution in a 500 mL bottle where the film was placed 1 cm above the ammonium solution. In the closed bottle, the films were exposed to the ammonium vapour for 20 min. Finally, the color parameters were determined.
- **Different pH solutions:** this experiment was carried out following the method described by (Li et al., 2019a) with slight modification. First, the films were cut in rectangles of (2 × 4 cm²) and then they were immersed in 10 mL of different solutions of pH 2, 4, 6, 8, 10, 12 and 14 (HCl 0.1 M and NaOH 0.1 M) for 30 min at 25 °C. Afterwards, they were dried at room temperature and the color parameters were determined.

Nanocomposite films without any treatment were used as control.

The halochromic variation of films, after their exposure to different pH and volatile ammonia, was evaluated using a colorimeter (PCE-CSM3, PCE, Spain) and the CIELAB color scale. The parameters measured were L*(brightness), b*(- blue to + yellow), a* (- green to + red) and the color difference (ΔE*). This last parameter was calculated using the following equation (Mujtaba et al., 2017):

$$\Delta E^* = \sqrt{[(\Delta L^*)^2 + (\Delta a^*)^2 + (\Delta b^*)^2]} \quad (4)$$

The measurements were obtained in 10 random sections of each sample and the results were expressed as average and standard deviation.

2.6.4. Total phenolic content and antioxidant activity

The total phenolic content (TPC) was carried out according to the procedure described by Fernández-Marín et al. with slight modifications (Fernández-Marín, Labidi, et al., 2020). The samples were prepared by weighting 25 mg of each following by their immersion in 3 mL of methanol (MeOH). The mixture was centrifuged for 24 h at 500 rpm and then 300 µL of the solution was collected. Absorption at 760 nm was measured with an UV/Vis spectrophotometer (Jasco V-730, Pfungstadt,

Germany) using gallic acid as a standard. The results were expressed in mg gallic acid equivalents (mg GAE/g films) and three replicates were performed for each sample.

The antioxidant activity of the nanocomposite films was assessed by DPPH (2, 2-diphenyl-1-picrylhydrazyl) free radical scavenging activity assay (Fernández-Marín, Fernandes, Andrés, & Labidi, 2021). First, 25 mg of each sample was weighted and immersed in 3 mL of MeOH, which was centrifuged for 24 h at 500 rpm. Supernatant was collected (300 μ L) and mixed with 3 mL of a solution of 6×10^{-5} M DPPH dissolved in MeOH. The absorbance at 515 nm was measured with an UV/Vis spectrophotometer (Jasco V-630, Pfungstadt, Germany) after 15 min and Trolox was used as standard. The results were expressed as the percentage of DPPH radical scavenging activity according to the following equation (5):

$$DPPH \% = \frac{A_0 - A_S}{A_0} \times 100 \quad (5)$$

where A_0 represents the absorbance of DPPH of the control and A_S corresponds to the absorbance of the film. Each sample was measured in triplicate.

2.6.5. Statistical analysis

A one-way analysis of variance (ANOVA) statistical test was performed using SPSS software (version 24, Inc. Chicago, IL, USA). Significant difference values were obtained by Duncan's multiple range test. The results were expressed as average and standard deviation. P-values < 0.05 were statistically significant.

3. Results and discussion

3.1. General aspect and properties of the nanocomposite films

The general aspect of food packaging and its optical properties like color, opacity and transmittance are a very important factor for both consumer acceptance and food protection against photodegradation (Alizadeh-Sani et al., 2021; Ezati & Rhim, 2020). Fig. 1 displays the general aspect of the final nanocomposite films. As shown in Fig. 1, the samples are translucent and homogeneous and the nanocomposite films with bioactive agent's exhibit yellowish, orange and brownish colors (see also Fig. 2, Table 4 and section 3.2.1.). The thicknesses and grammage of the biocomposite films are shown in Table 2. The data revealed that the different thickness values are correlated with the grammage and further depend on the phenolic compounds that are bound to the chitosan matrix (de Jesus, Baldasso, Marcflio, & Tessaro, 2020; Khoshgozaran-Abras, Azizi, Hamidy, & Bagheripoor-Fallah, 2012; J. Liu, Wang, et al., 2019; Sani, Pirsra, & Tağı, 2019).

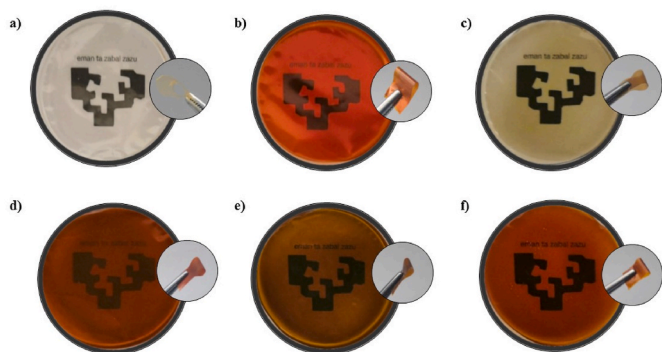


Fig. 1. Photographs showing the general aspect and the flexibility of the films. a) CSNC; b) CSNC-C; c) CSNC-A; d) CSNC-CA(8:1); e) CSNC-CA(1:8); f) CSNC-CA(1:1).

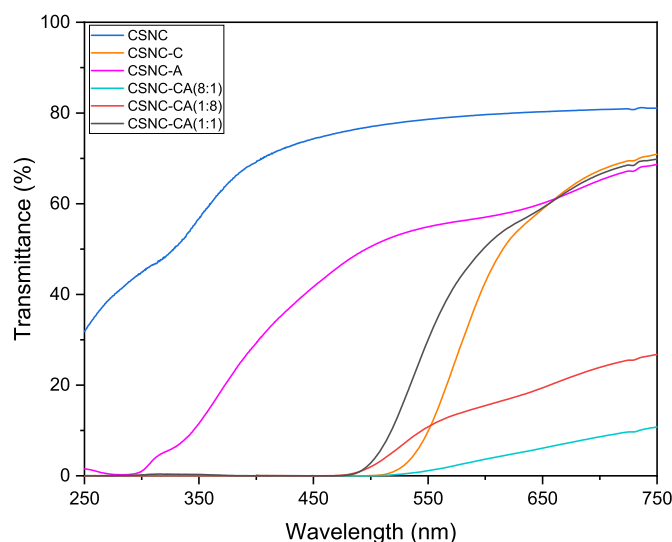


Fig. 2. Transmittance from 750 to 250 nm of nanocomposite films.

Table 2

Thickness, grammage, MC (moisture content), WS (water solubility) and opacity of the films.

Samples	Thickness (μ m)	Grammage (g/m^2)	MC %	WS %	Opacity
CSNC	49.67 \pm 2.07 ^a	56.07 \pm 6.70 ^a	41.73 \pm 0.69 ^a	48.50 \pm 1.08 ^a	4.18 \pm 0.20 ^{ab}
CSNC-C	58.67 \pm 2.16 ^b	68.01 \pm 5.46 ^b	22.88 \pm 1.28 ^b	29.46 \pm 0.97 ^b	6.81 \pm 0.56 ^b
CSNC-A	49.00 \pm 1.79 ^a	53.93 \pm 3.01 ^c	34.20 \pm 1.37 ^c	41.88 \pm 0.88 ^c	6.73 \pm 2.76 ^b
CSNC-CA (8:1)	49.83 \pm 2.64 ^a	60.37 \pm 5.89 ^d	25.39 \pm 1.35 ^d	31.44 \pm 0.86 ^c	29.39 \pm 2.10 ^c
CSNC-CA (1:8)	47.17 \pm 1.33 ^c	48.37 \pm 4.20 ^e	32.49 \pm 1.61 ^c	38.85 \pm 0.92 ^d	18.67 \pm 0.73 ^d
CSNC-CA (1:1)	47.50 \pm 3.94 ^c	48.74 \pm 1.22 ^e	27.78 \pm 1.35 ^e	35.57 \pm 1.64 ^e	6.28 \pm 0.98 ^b

Values are expressed as mean \pm standard deviation (thickness n = 6; moisture content, water solubility and opacity n = 3). Different letters in the same column denote significant differences between films (Duncan's test, p < 0.05).

3.1.1. Light transmission and opacity

As defined before, the opacity (Table 2) of the films was measured at 600 nm (Fig. 2) and taking in account the thickness of the samples (Table 2). As expected, it was observed that the CSNC nanocomposite film (control) showed the lowest value (4.18 ± 0.20). Higher opacities were observed in the films with prepared with a mixture of curcuma oil and anthocyanin, exhibiting the greatest value when the proportion of curcuma was higher (CSNC-CA(8:1): 29.39 ± 2.10). This may be due to the absorption of some of the light by the mixture of its chromophores and also agrees with the data observed in Fig. 2 for transmittance (Alizadeh-Sani et al., 2021).

Fig. 2 shows the transmittance of the nanocomposite films from 250 to 750 nm (UV-Vis light). As expected, the incorporation of curcuma oil and anthocyanin into the nanocomposite films decrease their transmittance; and, interestingly, the spectra profile differ depending the kind of additive or mixture. All films containing curcuma oil showed a drastic decrease in transmittance around 500 nm, showing to be a great barrier against UV radiation, probably due to the presence of phenolic compounds (Xinhui Zhang et al., 2021). The CSNC-CA(8:1) and CSNC-CA(1:8) nanocomposite films exhibited very low transmittance in the visible region and a total blocking in the UV region.

For food packaging films, another important characteristic is their behaviour towards moisture and water.

3.1.2. Water solubility and moisture content

Table 2 shows the water solubility (WS) data of the biocomposite films. CSNC film (chitosan and chitin nanocrystals) showed a WS value of $48.50 \pm 1.08\%$. This value was much lower than pure CS film obtained by (Kaya, Ravikumar, et al., 2018) with a WS value of 73%, due to its hydrophilic nature. This result showed that the addition of nanocrystals decrease the water solubility of the films. The addition of curcuma oil and anthocyanins improved the WS properties with respect to the CSNC control film ($p < 0.05$). However, the incorporation of anthocyanin, due to its hydrophilic nature, showed slightly higher values than in the films with higher curcuma oil content. This was confirmed in the CSNC-C film, which showed the lowest WS value. This is mainly due to the fact that most of the compounds in the oil have hydrophobic properties (Xinhui Zhang et al., 2021).

The moisture content (MC) values are listed in Table 2. The data revealed that the presence of curcuma oil and anthocyanins decrease the MC of the samples. Other authors, who added essential oils and nanofibres in chitosan films, or purple-fleshed sweet potato extract also observed the same behaviour (Pereda, Dufresne, Aranguren, & Marco-vich, 2014; Yong, Wang, Bai, et al., 2019). Both films with anthocyanin extracts and curcuma oil significantly decreased the MC values since they can form bonds with the hydroxyl or amino groups of CS preventing their interaction with water (Ojagh Mahdi, Rezaei, Razavi Hadi, Mohamad, & Hosseini, 2010; Yong, Wang, Bai, et al., 2019). It was also observed that the films with the highest curcuma oil content (CSNC and CSNC-CA(8:1)) showed the lowest values, possibly due to their high content of non-polar compounds (X. Chen et al., 2017).

3.1.3. Water contact angle

The water contact angle technique evaluates the hydrophilic or hydrophobic behaviour of the materials. Films with angles greater than 90° are considered hydrophobic (Hajji et al., 2021). To assess the hydrophilic or hydrophobic character of the nanocomposite films, the contact angle was measured at 0 s and 120 s after to depose a water drop at the surface of the films. The data displayed in Fig. 3 is in accordance with the data obtained by the water sensitive tests described before. The addition of α -CHNC slightly improved the water contact angle of the nanocomposite film with respect to pure chitosan films which are usually in the range of $69\text{--}85^\circ$ ($t = 0$) as shown by numerous works such as (Cunha et al., 2008; Dresvyanina et al., 2021; Kaya, Salaberria, et al., 2018; Souza et al., 2014): nonetheless, CSNC films still showing hydrophilic properties over time, i.e., the water contact angle decrease

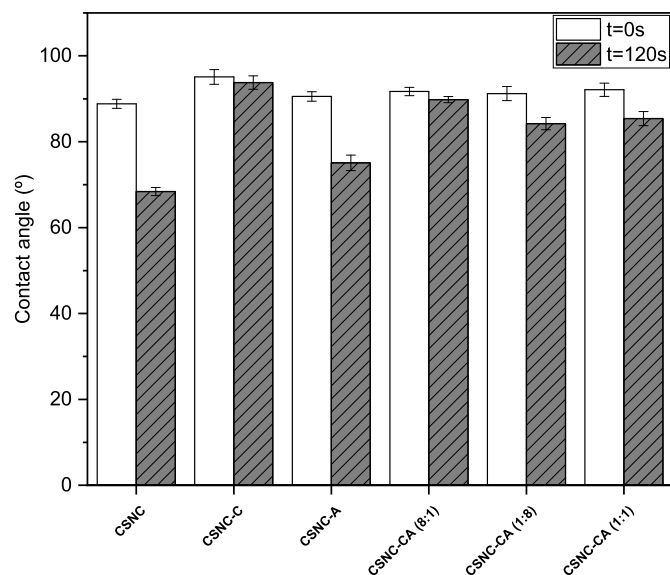


Fig. 3. Water contact angle of the nanocomposite films at 0 and 120 s.

from 88° for $t = 0$ to 68.4° at 120 s. On the other hand, the addition of curcuma oil improved their hydrophobic properties as they exhibited angles greater than 90° ($t = 0$). The films CSNC-C and CSNC-CA(8:1) exhibited lower contact angle loss ($\Delta\alpha = 1.3$ and 1.9, respectively) after the 120 s as this curcuma oil contains high percentage of non-polar compounds such as Ar-turmerone, turmerone and β -turmerone revealing its hydrophobic nature (Kaya, Ravikumar, et al., 2018). The films prepared with anthocyanins (CSNC-A; CSNC-CA(1:8) and CSNC-CA(1:1)) showed a decrease in the contact angle after 120 s. This is explained by the fact that they contain a large number of hydroxyl groups which can form hydrogen bonds with water, thus demonstrating their affinity for water (S. Chen, Zhang, et al., 2020).

3.2. Mechanical properties

Because of the handling, transport and storage of packaging material for food, another important characteristic of these materials is their mechanical properties (Kanatt, Rao, Chawla, & Sharma, 2012). The mechanical properties of the nanocomposite films were shown in Table 3.

In general, the addition of curcuma oil and anthocyanins significantly improved the breaking resistance. And, it was also observed that both CSNC-A and CSNC-CA(1:8) films, which contain the highest proportion of anthocyanins, exhibited the highest TS values. This may be due to the formation of a more stable interactions between CS chains and CHNC and the other additives into the film (Qianyun Ma & Wang, 2016; Yong & Liu, 2020). The YM follows the same trend found for the TS parameter. The incorporation of curcuma oil, anthocyanin extract and their mixture increased the YM, showing the highest value in the CSNC-CA(1:8) nanocomposite film with 63.94 ± 9.07 MPa. These results are probably due to the adhesion between the matrix and the anthocyanin extract at the interface since both are hydrophilic (Qinyan Ma et al., 2019; Roy & Rhim, 2021). On the other hand, significant decrease in E % occurred with the addition of the bioactive compounds. This behaviour was also found by authors such as Zhou X. et al., in their study based on konjac glucomannan and camellia oil films with the addition of carrageenan, anthocyanin extracts and curcumin (Zhou et al., 2021). Li Y. et al., reported this trend in chitosan films reinforced with deacetylated chitin nanofibers and purple potato extraction by increasing the concentration of nanofibers (Li et al., 2019a). These results may be due to the interactions formed by the extracts and the matrix, which impedes the CS-CS interaction reducing the flexibility of the film (Roy & Rhim, 2021; Yong & Liu, 2020; Zhou et al., 2021). Overall, the mixture of anthocyanins and curcuma oil improved the mechanical properties which is in agreement with the results obtained by (Zhou et al., 2021).

3.3. TGA

The influence of the introduction of anthocyanins and curcuma oil on the CSNC nanocomposite films was evaluated by thermogravimetric analysis and the TGA and the derivative DTG curves are shown in Fig. 4. In general, all nanocomposite films displayed profiles with 3 main degradation steps. The first step of degradation occurred below 100°C

Table 3

Mechanical properties of the nanocomposite films: TS (tensile strength, MPa), YM (Young's modulus, MPa), E (elongation, %). Values are mean \pm standard deviation ($n = 6$). The superscript letters in the same column denote significant differences among the nanocomposite films (Duncan's test, $p < 0.05$).

	TS (MPa)	YM (MPa)	E (%)
CSNC	19.52 ± 4.92^a	31.31 ± 1.29^a	29.79 ± 9.91^a
CSNC-C	26.94 ± 2.87^b	36.04 ± 3.13^b	27.52 ± 8.14^b
CSNC-A	28.92 ± 1.46^c	52.67 ± 4.83^c	18.76 ± 1.17^c
CSNC-CA(8:1)	24.80 ± 1.89^d	46.99 ± 7.11^d	32.62 ± 4.73^d
CSNC-CA(1:8)	30.55 ± 3.55^e	63.94 ± 9.07^e	21.45 ± 1.92^e
CSNC-CA(1:1)	25.42 ± 2.29^{bd}	34.01 ± 1.46^b	15.44 ± 7.54^f

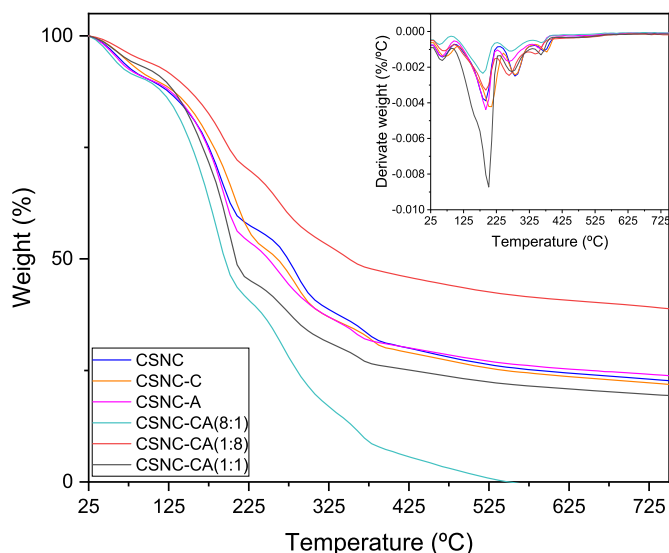


Fig. 4. TGA and dTG profiles of the nanocomposite films.

and was due to the evaporation of water and acetic acid residue (Xin Zhang, Zou, et al., 2019). In the second step, the onset temperatures were between 125 and 150 °C with a maximum degradation between 200 and 225 °C and were assigned to the loss of the low molecular weight molecules of the anthocyanins and curcuma oil and glycerol molecules (Alizadeh-Sani et al., 2021; Silva Damasceno et al., 2018). The third step was observed between 275 and 325 °C and were attributed to the chitosan and nanochitin degradation. In addition, some degradation of curcuma oil and anthocyanin extracts can also occur in this step (Shen & Kamdem, 2015; Xin Zhang, Zou, et al., 2019). In general, the results indicated that the addition of curcuma oil and anthocyanin extract exhibited lower thermal stability than the pure CSNC nanocomposite films. This type of behaviour has also been observed by other authors such as Silva-Pereira M. C. et al., who studied CS and corn starch films by adding red cabbage extract (Silva-Pereira, Teixeira, Pereira-Júnior, & Stefani, 2015). This effect may be explained by the fact that the incorporated additives reduce the intramolecular interactions between the different components of the film matrix (Kim, Baek, & Song, 2018; Silva-Pereira et al., 2015; Yong, Wang, Bai, et al., 2019).

3.4. pH- and volatile ammonia-sensitivity

As mentioned before, in order to evaluate the halochromic capacity of the samples, the films were first exposed to pH-variations and volatile ammonia and then their color was measured. The colors of the untreated films was also measured and used as control.

3.4.1. Color of untreated films

The color parameters L^* , a^* , b^* and ΔE of the untreated films are shown in Table 4. In the L^* parameter it can be seen that the CSNC films showed values close to 90 so they tend to lightness ($p > 0.05$). While the films containing the bioactive agents are darker than the control CSNC film. In the parameter a^* , which indicates -green/+red, it was observed that all films trended towards red as they have a positive sign. The parameter a^* increased due to the influence of curcuma oil ($p < 0.05$). These results are in agreement with those obtained previously in films prepared with poly(vinyl alcohol), curcumin and grapefruit seed extract (Roy & Rhim, 2021). The same trend was observed for the parameter b^* (-blue/+yellow). The films with the bioactive compounds showed a tendency to yellow. The CSNC-C film showed the highest values of a^* and b^* parameters being 32.66 ± 0.11 and 46.37 ± 1.98 , respectively. The mixture of both parameters was reflected in the appearance of the

film shown in Table 4. The addition of curcuma oil and anthocyanin extract significantly ($p < 0.05$) affected the total color difference (ΔE) of the films.

3.4.2. Color of the samples treated with volatile ammonia

The sensitivity of the films to ammonium gases was assessed by color variation at two different concentrations: 0.08 mol/L and 0.5 mol/L (Table 5). This experiment is useful because simulates the films sensitivity to volatile compounds generated in the meat decomposition. The mechanism that possibly occurs is that ammonia gas diffuses through the film matrix and is hydrolysed generating hydroxyl ions producing an alkaline environment for the film (Yun et al., 2019; J.; Zhang, Zou, et al., 2019). This causes that the anthocyanin and curcumin pigments, change the structure and consequently the color (Sahne et al., 2017; Yun et al., 2019). In all films the data showed positive values of a^* and b^* parameters indicating that the colors were going to reds and yellows.

All the nanocomposite films were translucent and homogeneous showing a good uniformity of the colors. In the CSNC-C film, it was observed that increasing the ammonium concentration increased the parameter a^* and decreased b^* ($p < 0.05$) in comparison with the untreated film, so that the tendency of the film color was red and less yellow. As for the CSNC-A film, a considerable increase in a^* and b^* was observed, which could be observed by the changing of the color from yellow to brown. Furthermore, no significant difference was observed regarding the change of ammonia concentrations ($p > 0.05$). In the CSNC-CA(8:1) and CSNC-CA(1:8) films the L^* and a^* parameters are similar while a greater change in the b^* parameter was observed. The highest b^* values were found in the CSNC-CA(1:8) film, which contains a higher amount of anthocyanin and therefore tends to yellow. Regarding the CSNC-CA(1:1) film, no significant differences were observed in the parameters L^* , a^* , b^* and ΔE when they were subjected to the two ammonia concentrations ($p > 0.05$). However, it was observed that the b^* parameter was somewhat higher and tended more strongly to yellow color when exposed to higher ammonium concentration. In general, all films demonstrated sensitivity to ammonia gas exposure and no significant difference was observed between the two concentrations. These results demonstrated that the films could be employed for food packaging as indicators of food degradation.

3.4.3. Color of the samples at different pH



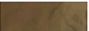







The films were exposed to different pH dilutions and their halochromic capacity is shown in Table 6. In general, the samples showed to be translucent and homogeneous showing a good uniformity of the color in the films. The color of the CSNC-C film became darker (L^*), redder (a^*) and less yellowish (b^*) as the pH became more basic. This is because the pigment curcumin changes structure to the enol form predominantly

Table 4
Color parameters of normal untreated nanocomposite films.

	Normal color of the films				Appearance
	L^*	a^*	b^*	ΔE	
CSNC	93.85 ± 0.28^a	0.20 ± 0.03^a	-0.75 ± 0.19^b	0.92 ± 0.16^b	
CSNC-C	56.54 ± 0.46^b	32.66 ± 0.11^b	46.37 ± 1.98^c	71.15 ± 0.57^c	
CSNC-A	72.36 ± 0.77^c	1.15 ± 0.13^c	12.23 ± 0.44^d	24.96 ± 0.77^d	
CSNC-CA (8:1)	43.93 ± 0.25^d	21.19 ± 0.61^d	24.10 ± 0.53^e	59.52 ± 0.25^e	
CSNC-CA (1:8)	44.06 ± 0.45^d	16.32 ± 0.11^e	26.04 ± 0.75^f	58.71 ± 0.13^f	
CSNC-CA (1:1)	47.21 ± 0.96^e	32.64 ± 0.33^b	31.87 ± 1.58^g	65.65 ± 0.46^g	

The values were average \pm standard deviation (normal color of the films, $n = 10$). In the analysis of the normal color of the films: the superscript letters in the same column indicate the significant differences between each parameter and the films (Duncan's test, $p < 0.05$).

Table 5
Color parameters of nanocomposite films treated with volatile ammonia.

Color of films exposed to ammonia gases					
	L*	a*	b*	ΔE	Appearance
CSNC-C					
0.08 mol/L	47.74 ± 2.23	35.58 ± 0.37 ^a	35.77 ± 1.18 ^a	68.66 ± 0.97 ^a	
NH ₃	0.23 ^a	0.37 ^a	1.18 ^a	0.97 ^a	
0.5 mol/L	42.88 ± 1.33 ^b	40.70 ± 0.86 ^b	27.82 ± 1.22 ^b	70.86 ± 0.95 ^a	
NH ₃	1.33 ^b	0.86 ^b	1.22 ^b	0.95 ^a	
CSNC-A					
0.08 mol/L	68.55 ± 0.16 ^a	11.08 ± 0.37 ^a	31.47 ± 2.23 ^a	42.08 ± 1.90 ^a	
NH ₃	0.16 ^a	0.37 ^a	2.23 ^a	1.90 ^a	
0.5 mol/L	64.44 ± 1.32 ^b	14.77 ± 0.69 ^a	35.67 ± 0.49 ^a	48.73 ± 0.99 ^b	
NH ₃	1.32 ^b	0.69 ^a	0.49 ^a	0.99 ^b	
CSNC-CA(8:1)					
0.08 mol/L	34.78 ± 1.23 ^a	22.76 ± 2.11 ^a	10.40 ± 1.44 ^a	63.80 ± 0.11 ^a	
NH ₃	1.23 ^a	2.11 ^a	1.44 ^a	0.11 ^a	
0.5 mol/L	40.77 ± 1.06 ^b	24.21 ± 1.27 ^a	18.60 ± 1.32 ^b	61.02 ± 0.04 ^a	
NH ₃	1.06 ^b	1.27 ^a	1.32 ^b	0.04 ^a	
CSNC-CA(1:8)					
0.08 mol/L	42.52 ± 0.07 ^a	22.20 ± 0.35 ^a	27.39 ± 0.66 ^a	62.12 ± 0.13 ^a	
NH ₃	0.07 ^a	0.35 ^a	0.66 ^a	0.13 ^a	
0.5 mol/L	40.89 ± 2.16 ^a	32.01 ± 1.45 ^b	24.60 ± 1.65 ^a	66.47 ± 1.78 ^a	
NH ₃	2.16 ^a	1.45 ^b	1.65 ^a	1.78 ^a	
CSNC-CA(1:1)					
0.08 mol/L	43.57 ± 0.30 ^a	34.34 ± 0.28 ^a	25.27 ± 0.70 ^a	65.82 ± 0.65 ^a	
NH ₃	0.30 ^a	0.28 ^a	0.70 ^a	0.65 ^a	
0.5 mol/L	46.08 ± 1.11 ^a	36.46 ± 0.19 ^a	32.37 ± 2.21 ^a	68.28 ± 0.47 ^a	
L NH ₃	1.11 ^a	0.19 ^a	2.21 ^a	0.47 ^a	

The values were average ± standard deviation (n = 10). In the color analysis of films exposed to ammonia gas: the letters superscript represent the significant differences between the two different concentrations of ammonia gas and each parameter of each film (Duncan's test, p < 0.05).

at basic pH (H. zhi [Chen, Zhang, et al., 2020](#)). In the CSNC-A film, it showed at pH = 2 a reddish color due to its a* parameter (35.23 ± 0.45) and the change of the anthocyanin structure to the flavylum form ([Sigurdson, Robbins, Collins, & Giusti, 2019](#); [Yong, Wang, Bai, et al., 2019](#)). At pH = 4, a drop in the a* value was observed which contributed to the film appearing more yellowish. Between pH = 6–10 no significant changes between the parameters were found and a dark greenish color was observed. This resulted in no visible change in color with the naked eye. From pH = 12 an increasing b* and L* value was noticed which resulted in a bright yellowish color. This color trend was also observed by [Yong H. et al.](#) in their analysis of chitosan films with purple-fleshed sweet potato extract ([Yong, Wang, Bai, et al., 2019](#)). As for the films with mixed curcumin oil and anthocyanin, the perceived colors were more similar to those of curcuma oil. Similar results were observed in the study of [Chen H. et al., 2019](#), who mixed curcumin and anthocyanins in the matrix of starch, poly(vinyl alcohol) and glycerol (H. zhi [Chen, Zhang, et al., 2020](#)). In general, all films regardless of pH exhibited a tendency towards dark shades, with L* values being less than 50. In addition, most of them were observed to have ΔE values between 60 and 70. The CSNC-CA(8:1) film revealed orange to reddish tones due to the higher proportion of curcuma oil. These results are reflected by the increase of parameter a* and the decrease of b* as the pH becomes more basic. As for the CSNC-CA(1:8) film, it was found that the a* parameter gradually increased as the pH approached 14. In the colors of these films, the major presence of the anthocyanin extract was observed. Between pH = 2–8 the b* values were higher than the a* values, which was reflected in yellowish-brownish colors. When the pH becomes more basic, between 10 and 12, the films turned more yellow due to the increase of b*. It is worth noting that at pH = 14 the film showed a dark red color due to the drastic increase of the a* parameter (32.812 ± 0.83). Finally, the colors observed in the CSNC-CA(1:1) film varied from yellow to reddish-orange. Between pH = 4–6, the film redness (a* values) increased while the yellowness (b* values) decreased. On the other hand, a color change to brown tones was obtained between pH = 8–12

showing similar a* and b* values. Finally, it is important to underline that at pH = 14 the a* value rose significantly which gave an orange color to the film.

Interestingly, the color parameters of nanocomposite films prepared with the mixture of CSNC-CA(8:1) showed to be similar after their basic pH (10–12) exposure and volatile ammonia treatment. Thus, these color changes at different pH could be useful as an indicator in food packaging.

3.5. Total phenolic content and antioxidant activity

The antioxidant activity of the nanocomposite films is very important to prevent food oxidation and hence to extend the quality of the product. This was one of the motivations to add curcuma oil into the nanocomposite films with anthocyanins. In this work, first the total phenolic content (TPC) was assessed and then, the antioxidant properties were evaluated by DPPH free radical scavenging activity assay. The TPC assay determines the amount of total phenolic compounds contained in the samples, which are responsible of the antioxidant activity. The DPPH assay evaluates the substance capability of donating H to the free radical DPPH* ([Fernández-Marín, M. Fernandes et al., 2020](#); [Kanatt et al., 2012](#)). The TPC and DPPH scavenging activity data are listed in [Table 7](#).

Regarding the TPC, it was observed that the nanocomposite film prepared with curcuma oil (CSNC-C) exhibited higher TPC values than the CSNC nanocomposite films and those prepared with anthocyanins (CSNC-A) (p < 0.05). Interestingly, the nanocomposite films prepared with the mixture of both bioactive compounds presented the higher TPC values, being the CSNC-CA(8:1) film the one that showed the highest value.

These results were in agreement with those obtained by the DPPH assay to assess the antioxidant activity. In other words, it was observed that the mixture of curcuma oil and anthocyanin extract enhanced the antioxidant activity of the final CSNC nanocomposite films (p < 0.05). This could be explained since both curcuma oil but also anthocyanins contain phenolic compounds with the ability to donate hydrogen atoms ([Roy & Rhim, 2021](#); [Xinhui Zhang et al., 2021](#)). As expected, the CSNC-CA(8:1) film, which was prepared with the higher proportion of curcuma oil, showed the highest DPPH % value (76.10 ± 1.79%) ([de Carvalho et al., 2020](#); [Fernández-Marín, Fernandes, Andrés, & Labidi, 2021](#)). Therefore, the data revealed that these films could be used as film packaging to prevent food oxidation.

4. Conclusions

The aim of this study was to develop smart multifunctional materials based on chitosan/chitin nanocrystals nanocomposite films and curcuma oil and anthocyanins as pH- and volatile ammonia-sensitive agents. In general, the addition of curcuma oil and anthocyanin extract decreased the moisture content and water solubility of the nanocomposite films and improved their UV-Vis light barrier and mechanical properties. The halochromic and antioxidant properties of the films were assessed, and it was observed that the final materials are multifunctional since they are at the same time pH- and volatile ammonia-sensitive and present antioxidant properties. In general, the films with the bioactive compounds were sensible to the color change generated by the exposure to ammonium gas, and no significant differences were observed between the different concentrations used. As for the exposure to different pH solutions (2–14), changes were found in all the films with bioactive agents with greater changes in films with a higher percentage of curcuma oil (CSNC-C and CSNC-CA(8:1)). Interestingly, the nanocomposite film prepared with the mixture of CA(8:1) presented the best conditions for food preservation by presenting a great barrier to UV light, excellent antioxidant properties and halochromic capacity to both pH- and volatile ammonia changes. These results demonstrated that the use of the mixture of curcuma oil and

Table 6
Color parameters of films in pH solutions (2–14).

	pH		L*	a*	b*	ΔE	Appearance
CSNC-C	Acid	2	53.69 ± 2.50 ^a	29.39 ± 3.34 ^a	40.02 ± 3.16 ^a	49.79 ± 0.99 ^a	
		4	45.04 ± 0.93 ^b	36.25 ± 0.47 ^b	20.80 ± 0.01 ^b	41.79 ± 0.42 ^b	
	Neutral	6	49.09 ± 0.18 ^c	33.46 ± 0.10 ^c	33.62 ± 0.39 ^c	47.43 ± 0.34 ^c	
		8	44.33 ± 1.68 ^b	37.78 ± 1.80 ^b	26.26 ± 0.37 ^d	44.4 ± 3.56 ^d	
	Basic	10	41.59 ± 0.98 ^d	35.10 ± 0.35 ^d	17.18 ± 0.56 ^e	39.08 ± 0.57 ^d	
		12	40.25 ± 0.59 ^d	34.28 ± 0.86 ^d	14.91 ± 1.24 ^e	37.39 ± 1.29 ^d	
	14	39.62 ± 0.48 ^e	44.35 ± 0.67 ^e	20.12 ± 0.26 ^b	48.71 ± 0.71 ^a		
CSNC-A	Acid	2	50.43 ± 1.14 ^a	35.23 ± 0.45 ^a	32.45 ± 1.09 ^a	64.65 ± 0.45 ^{ab}	
		4	56.91 ± 1.49 ^b	12.93 ± 0.30 ^b	28.18 ± 0.11 ^b	48.65 ± 1.20 ^b	
	Neutral	6	47.79 ± 0.62 ^c	7.02 ± 0.11 ^c	24.63 ± 0.15 ^c	53.82 ± 0.47 ^a	
		8	46.80 ± 4.70 ^c	6.00 ± 0.10 ^{cd}	23.11 ± 1.29 ^c	53.73 ± 3.24 ^a	
	Basic	10	47.53 ± 1.70 ^c	6.27 ± 0.21 ^c	23.59 ± 1.50 ^c	53.48 ± 0.76 ^a	
		12	60.68 ± 0.52 ^b	4.84 ± 0.72 ^d	28.07 ± 0.94 ^d	45.00 ± 0.31 ^c	
	14	81.90 ± 0.15 ^d	6.10 ± 0.09 ^{cd}	34.01 ± 0.13 ^d	32.44 ± 0.12 ^d		
CSNC-CA(8: 1)	Acid	2	45.56 ± 0.06 ^a	19.72 ± 0.11 ^{ab}	24.08 ± 0.27 ^a	57.76 ± 0.13 ^a	
		4	41.81 ± 0.36 ^{bc}	15.40 ± 0.24 ^a	22.78 ± 1.56 ^b	58.75 ± 0.18 ^{ab}	
	Neutral	6	40.11 ± 0.51 ^{bc}	24.16 ± 0.83 ^{cd}	17.41 ± 1.65 ^b	62.34 ± 0.37 ^{ab}	
		8	40.76 ± 0.42 ^b	22.23 ± 0.16 ^{bc}	17.16 ± 0.28 ^b	60.08 ± 0.22 ^{bc}	
	Basic	10	40.62 ± 0.96 ^{ab}	25.10 ± 0.10 ^d	20.46 ± 0.38 ^a	64.06 ± 0.64 ^c	
		12	37.43 ± 0.40 ^b	22.31 ± 0.18 ^{ab}	13.17 ± 0.23 ^c	61.90 ± 0.26 ^{ab}	
	14	33.15 ± 0.33 ^c	27.56 ± 0.91 ^d	9.52 ± 0.37 ^d	68.06 ± 0.13 ^d		
CSNC-CA(1:8)	Acid	2	45.93 ± 0.02 ^a	19.29 ± 0.05 ^a	30.77 ± 0.22 ^a	61.23 ± 0.35 ^a	
		4	39.50 ± 0.06 ^{ab}	19.17 ± 0.40 ^{ab}	22.09 ± 0.30 ^a	62.76 ± 0.31 ^a	
	Neutral	6	43.27 ± 0.47 ^{cd}	18.20 ± 0.45 ^b	23.48 ± 2.13 ^a	58.83 ± 0.64 ^a	
		8	44.25 ± 0.19 ^{cd}	20.45 ± 0.37 ^c	27.09 ± 0.46 ^a	60.35 ± 0.50 ^a	
	Basic	10	49.86 ± 3.50 ^e	21.53 ± 0.40 ^c	35.48 ± 2.90 ^b	61.74 ± 0.97 ^b	
		12	44.16 ± 1.29 ^d	22.95 ± 0.15 ^c	27.22 ± 1.82 ^a	61.20 ± 0.25 ^a	
	14	36.05 ± 0.25 ^a	32.812 ± 0.83 ^d	16.45 ± 1.19 ^a	68.50 ± 0.50 ^a		
CSNC-CA(1: 1)	Acid	2	54.99 ± 0.51 ^a	23.46 ± 0.08 ^a	45.59 ± 0.66 ^a	65.60 ± 0.19 ^a	
		4	39.99 ± 0.23 ^b	31.29 ± 0.36 ^b	21.46 ± 0.42 ^b	66.78 ± 0.21 ^b	
	Neutral	6	41.35 ± 1.01 ^c	34.35 ± 0.28 ^b	20.24 ± 0.53 ^b	66.06 ± 0.77 ^c	
		8	43.86 ± 0.52 ^d	22.02 ± 0.06 ^c	27.15 ± 0.25 ^c	61.24 ± 0.28 ^d	
	Basic	10	42.81 ± 0.65 ^d	22.62 ± 0.36 ^c	26.79 ± 1.30 ^d	62.97 ± 1.24 ^d	
		12	41.85 ± 0.57 ^{cd}	22.85 ± 0.64 ^c	27.33 ± 1.85 ^e	64.08 ± 1.52 ^d	
	14	44.62 ± 0.11 ^d	46.51 ± 0.03 ^d	30.97 ± 0.08 ^f	75.40 ± 0.13 ^e		

The values represents average ± standard deviation (n = 10). The different superscript letters denote the significant differences of each film between each parameter at the different pH.

anthocyanin extract in chitosan/chitin nanocrystals nanocomposite films could be applied to the food industry due to their food quality sensors capacity and biodegradability.

CRedit author statement

Rut Fernández-Marín: Conceptualization, Methodology, Visualization, Investigation, Writing - Original Draft. Susana C.M. Fernandes:

Supervision, Validation, Writing - Review & Editing. M^a Ángeles Andrés Sánchez: Formal analysis, Supervision. Jalel Labidi: Writing - Review & Editing, Funding acquisition.

Declaration of competing interest

The authors declare that they have no known competing financial interests or personal relationships that could have appeared to influence

Table 7

Values of total phenolic content (TPC, mg GAE/g film) and antioxidant activity (DPPH assay, radical scavenging activity %) of the films. Results were average \pm standard deviation (n = 3). The superscript letters in the same column indicate significant differences (Duncan's test, p < 0.05) between each sample.

Samples	TPC (mg GAE/g film)	DPPH %
CSNC	7.93 \pm 2.48 ^a	18.46 \pm 0.03 ^a
CSNC-C	110.27 \pm 1.94 ^b	71.01 \pm 0.64 ^b
CSNC-A	17.96 \pm 0.42 ^c	69.41 \pm 0.02 ^b
CSNC-CA(8:1)	168.73 \pm 1.18 ^d	76.10 \pm 1.79 ^c
CSNC-CA(1:8)	119.56 \pm 1.27 ^b	71.27 \pm 1.65 ^d
CSNC-CA(1:1)	65.45 \pm 1.27 ^e	69.44 \pm 1.67 ^b

the work reported in this paper.

Acknowledgments

The authors would like to thank the funding from the Basque Country Government (IT 1008–16). R. F. –M. acknowledge the financial support of the Basque Country Government (scholarship of young researchers training). S.C.M.F. is a recipient of an E2S UPPA MANTA E2S Partnership Chair (Marine Materials) sponsored by the French programme “Investissements d’Avenir” administered by the French National Research Agency (ANR-16-IDEX-IDEX). The authors wish to acknowledge the technical and human assistance received from SGIker (UPV/EHU/ERDF, EU), Spain.

References

Alizadeh-Sani, M., Tavassoli, M., McClements, D. J., & Hamishehkar, H. (2021). Multifunctional halochromic packaging materials: Saffron petal anthocyanin loaded-chitosan nanofiber/methyl cellulose matrices. *Food Hydrocolloids*, *111*(May 2020), 106237. <https://doi.org/10.1016/j.foodhyd.2020.106237>

de Carvalho, F. A. L., Munekata, P. E. S., Lopes de Oliveira, A., Pateiro, M., Domínguez, R., Trindade, M. A., et al. (2020). Turmeric (*Curcuma longa* L.) extract on oxidative stability, physicochemical and sensory properties of fresh lamb sausage with fat replacement by tiger nut (*Cyperus esculentus* L.) oil. *Food Research International*, *136*, Article 109487. <https://doi.org/10.1016/j.foodres.2020.109487>. June.

Chaaban, A., Gomes, E. N., Richardi, V. S., Martins, C. E. N., Brum, J. S., Navarro-Silva, M. A., et al. (2019). Essential oil from *Curcuma longa* leaves: Can an overlooked by-product from turmeric industry be effective for myiasis control? *Industrial Crops and Products*, *132*(February), 352–364. <https://doi.org/10.1016/j.indcrop.2019.02.030>

Chen, X., He, X., Zhang, B., Fu, X., Jane, J., & Huang, Q. (2017). Effects of adding corn oil and soy protein to corn starch on the physicochemical and digestive properties of the starch. *International Journal of Biological Macromolecules*, *104*, 481–486.

Chen, S., Wu, M., Lu, P., Gao, L., Yan, S., & Wang, S. (2020a). Development of pH indicator and antimicrobial cellulose nanofiber packaging film based on purple sweet potato anthocyanin and oregano essential oil. *International Journal of Biological Macromolecules*, *149*, 271–280. <https://doi.org/10.1016/j.ijbiomac.2020.01.231>

Chen, H. zhi, Zhang, M., Bhandari, B., & Yang, C. hui (2020). Novel pH-sensitive films containing curcumin and anthocyanins to monitor fish freshness. *Food Hydrocolloids*, *100*, 105438. <https://doi.org/10.1016/j.foodhyd.2019.105438>. October 2019.

Claverie, M., McReynolds, C., Petitpas, A., Thomas, M., & Fernandes, S. C. M. (2020). Marine-derived polymeric materials and biomimetics: An overview. *Polymers*, *12*(5). <https://doi.org/10.3390/POLYM12051002>

Cunha, A. G., Fernandes, S. C. M., Freire, C. S. R., Silvestre, A. J. D., Neto, C. P., & Gandini, A. (2008). What is the real value of chitosan's surface energy? *Biomacromolecules*, *9*(2), 610–614. <https://doi.org/10.1021/bm701199g>

Dresvyanina, E. N., Kodolova-Chukhontseva, V. V., Bystryov, S. G., Dobrovol'skaya, I. P., Vaganov, G. V., Smirnova, N. V., et al. (2021). Influence of surface morphology of chitosan films modified by chitin nanofibrils on their biological properties. *Carbohydrate Polymers*, *262*, 117917. <https://doi.org/10.1016/j.carbpol.2021.117917>. October 2020.

Ezati, P., & Rhim, J. W. (2020). pH-responsive chitosan-based film incorporated with alizarin for intelligent packaging applications. *Food Hydrocolloids*, *102*, 105629. <https://doi.org/10.1016/j.foodhyd.2019.105629>. November 2019.

Fernández-Marín, R., Fernandes, S.C.M., Andrés, M.A., & Labidi, J. (2021). Microwave-Assisted Extraction of *Curcuma longa* L. Oil: Optimization, Chemical Structure and Composition, Antioxidant Activity and Comparison with Conventional Soxhlet Extraction. *Molecules*, *26*(6), 1516. <https://doi.org/10.3390/molecules26061516>

Fernández-Marín, R., Fernandes, S. C., McReynolds, C., Labidi, J., & Sánchez Andrés, M.Á. (2020a). Chapter 22-Chitosan-based materials as templates for essential oils. In *Handbook of chitin and chitosan-volume 3: Chitina-and chitosan-based polymer materials for various applications* (pp. 689–720). Elsevier.

Fernández-Marín, R., Hernández-Ramos, F., Salaberria, A. M., Sánchez Andrés, M.Á., Labidi, J., & Fernandes, S. C. M. (2021a). Eco-friendly isolation and characterization of nanochitin from different origins by microwave irradiation: Optimization using response surface methodology. *International Journal of Biological Macromolecules*, *186* (July), 218–226. <https://doi.org/10.1016/j.ijbiomac.2021.07.048>

Fernández-Marín, R., Labidi, J., Andrés, M.Á., & Fernandes, S. C. M. (2020). Using α -chitin nanocrystals to improve the final properties of poly (vinyl alcohol) films with *Origanum vulgare* essential oil. *Polymer Degradation and Stability*, Article 109227. <https://doi.org/10.1016/j.polydegradstab.2020.109227>

Hajji, S., Kchaou, H., Bkhairia, I., Slama-Ben, R. B., Boufi, S., Debeaufort, F., et al. (2021). Conception of active food packaging films based on 1 crab chitosan and 2 gelatin enriched with crustacean protein hydrolysates with improved 3 functional and biological properties. *Food Hydrocolloids*, Article 135907. <https://doi.org/10.1016/j.foodhyd.2021.106639>

Halász, K., & Csóka, L. (2018). Black chokeberry (*Aronia melanocarpa*) pomace extract immobilized in chitosan for colorimetric pH indicator film application. *Food Packaging and Shelf Life*, *16*, 185–193. <https://doi.org/10.1016/j.foodpsl.2018.03.002>. February.

de Jesus, G. L., Baldasso, C., Marcílio, N. R., & Tessaro, I. C. (2020). Demineralized whey-gelatin composite films: Effects of composition on film formation, mechanical, and physical properties. *Journal of Applied Polymer Science*, *137*(42), 1–11. <https://doi.org/10.1002/app.49282>

Joseph, B., Sam, R. M., Balakrishnan, P., Maria, H. J., Gopi, S., Volova, T., et al. (2020). Extraction of nanochitin from marine resources and fabrication of polymer nanocomposites: Recent advances. *Polymers*, *12*(8). <https://doi.org/10.3390/POLYM12081664>

Kalpana, S., Priyadarshini, S. R., Maria Leena, M., Moses, J. A., & Anandharamkrishnan, C. (2019). Intelligent packaging: Trends and applications in food systems. *Trends in Food Science & Technology*, *93*, 145–157. <https://doi.org/10.1016/j.tifs.2019.09.008>. October 2018.

Kanatt, S. R., Rao, M. S., Chawla, S. P., & Sharma, A. (2012). Active chitosan e polyvinyl alcohol films with natural extracts. *Food Hydrocolloids*, *29*(2), 290–297. <https://doi.org/10.1016/j.foodhyd.2012.03.005>

Kasaai, M. R. (2010). Determination of the degree of N-acetylation for chitin and chitosan by various NMR spectroscopy techniques: A review. *Carbohydrate Polymers*, *79*(4), 801–810. <https://doi.org/10.1016/j.carbpol.2009.10.051>

Kaya, M., Ravikumar, P., Ilk, S., Mujtaba, M., Akyuz, L., Labidi, J., et al. (2018). Production and characterization of chitosan based edible films from *Berberis crataegina*'s fruit extract and seed oil. *Innovative Food Science & Emerging Technologies*, *45*, 287–297. <https://doi.org/10.1016/j.ifset.2017.11.013>. October 2017.

Kaya, M., Salaberria, A. M., Mujtaba, M., Labidi, J., Baran, T., Mulercikas, P., et al. (2018a). An inclusive physicochemical comparison of natural and synthetic chitin films. *International Journal of Biological Macromolecules*, *106*, 1062–1070. <https://doi.org/10.1016/j.ijbiomac.2017.08.108>

Khoshozaran-Abrams, S., Azizi, M. H., Hamidy, Z., & Bagheripoor-Fallah, N. (2012). Mechanical, physicochemical and color properties of chitosan based-films as a function of Aloe vera gel incorporation. *Carbohydrate Polymers*, *87*(3), 2058–2062. <https://doi.org/10.1016/j.carbpol.2011.10.020>

Kim, S., Baek, S. K., & Song, K. B. (2018). Physical and antioxidant properties of alginate films prepared from *Sargassum fulvellum* with black chokeberry extract. *Food Packaging and Shelf Life*, *18*, 157–163. <https://doi.org/10.1016/j.foodpsl.2018.11.008>. July.

Koshy, R. R., Koshy, J. T., Mary, S. K., Sadanandan, S., Jisha, S., & Pothan, L. A. (2021). Preparation of pH sensitive film based on starch/carbon nano dots incorporating anthocyanin for monitoring spoilage of pork. *Food Control*, *126*, 108039. <https://doi.org/10.1016/j.foodcont.2021.108039>. November 2020.

Liang, T., Sun, G., Cao, L., Li, J., & Wang, L. (2019). A pH and NH₃ sensing intelligent film based on *Artemisia sphaerocephala* Krasch. gum and red cabbage anthocyanins anchored by carboxymethyl cellulose sodium added as a host complex. *Food Hydrocolloids*, *87*, 858–868. <https://doi.org/10.1016/j.foodhyd.2018.08.028>. July 2018.

Liu, Y., Qin, Y., Bai, R., Zhang, X., Yuan, L., & Liu, J. (2019a). Preparation of pH-sensitive and antioxidant packaging films based on κ -carrageenan and mulberry polyphenolic extract. *International Journal of Biological Macromolecules*, *134*, 993–1001. <https://doi.org/10.1016/j.ijbiomac.2019.05.175>

Liu, J., Wang, H., Guo, M., Li, L., Chen, M., Jiang, S., et al. (2019). Extract from *Lycium ruthenicum* Murr. Incorporating κ -carrageenan colorimetric film with a wide pH-sensing range for food freshness monitoring. *Food Hydrocolloids*, *94*, 1–10. <https://doi.org/10.1016/j.foodhyd.2019.03.008>. February.

Li, Y., Ying, Y., Zhou, Y., Ge, Y., Yuan, C., Wu, C., et al. (2019a). A pH-indicating intelligent packaging composed of chitosan-purple potato extractions strength by surface-deacetylated chitin nanofibers. *International Journal of Biological Macromolecules*, *127*, 376–384. <https://doi.org/10.1016/j.ijbiomac.2019.01.060>

Ma, Q., Liang, T., Cao, L., & Wang, L. (2018). Intelligent poly (vinyl alcohol)-chitosan nanoparticles-mulberry extracts films capable of monitoring pH variations. *International Journal of Biological Macromolecules*, *108*, 576–584. <https://doi.org/10.1016/j.ijbiomac.2017.12.049>

Ma, Q., Pang, K., Wang, K., Huang, S., Ding, B., Duan, Y., et al. (2019). Ultrafine and carboxylated β -chitin nanofibers prepared from squid pen and its transparent hydrogels. *Carbohydrate Polymers*, *211*, 118–123. <https://doi.org/10.1016/j.carbpol.2019.02.001>. March 2018.

Ma, Q., & Wang, L. (2016). Preparation of a visual pH-sensing film based on tara gum incorporating cellulose and extracts from grape skins. *Sensors and Actuators B: Chemical*, *235*, 401–407. <https://doi.org/10.1016/j.snb.2016.05.107>

- Mizgier, P., Kucharska, A. Z., Sokół-Letowska, A., Kolniak-Ostek, J., Kidoń, M., & Fecka, I. (2016). Characterization of phenolic compounds and antioxidant and anti-inflammatory properties of red cabbage and purple carrot extracts. *Journal of Functional Foods*, 21, 133–146. <https://doi.org/10.1016/j.jff.2015.12.004>
- Mujtaba, M., Salaberria, A. M., Andres, M. A., Kaya, M., Gunyakti, A., & Labidi, J. (2017). Utilization of flax (*Linum usitatissimum*) cellulose nanocrystals as reinforcing material for chitosan films. *International Journal of Biological Macromolecules*, 104, 944–952. <https://doi.org/10.1016/j.ijbiomac.2017.06.127>
- Ojagh Mahdi, S., Rezaei, M., Razavi Hadi, S., Mohamad, S., & Hosseini, H. (2010). Development and evaluation of a novel biodegradable film made from chitosan and cinnamon essential oil with low affinity toward water. *Food Chemistry*, 122(1), 161–166. <https://doi.org/10.1016/j.foodchem.2010.02.033>
- Pereda, M., Dufresne, A., Aranguren, M. I., & Marcovich, N. E. (2014). Polyelectrolyte films based on chitosan/olive oil and reinforced with cellulose nanocrystals. *Carbohydrate Polymers*, 101(1), 1018–1026. <https://doi.org/10.1016/j.carbpol.2013.10.046>
- Pereira, V. A., de Arruda, I. N. Q., & Stefani, R. (2015). Active chitosan/PVA films with anthocyanins from Brassica oleraceae (Red Cabbage) as Time-Temperature Indicators for application in intelligent food packaging. *Food Hydrocolloids*, 43, 180–188. <https://doi.org/10.1016/j.foodhyd.2014.05.014>
- Roy, S., & Rhim, J. W. (2021). Antioxidant and antimicrobial poly(vinyl alcohol)-based films incorporated with grapefruit seed extract and curcumin. *Journal of Environmental Chemical Engineering*, 9(1), 104694. <https://doi.org/10.1016/j.jece.2020.104694>
- Sagheer, F. A. A., Al-Sughayer, M. A., Muslim, S., & Elsabee, M. Z. (2009). Extraction and characterization of chitin and chitosan from marine sources in Arabian Gulf. *Carbohydrate Polymers*, 77(2), 410–419. <https://doi.org/10.1016/j.carbpol.2009.01.032>
- Sahne, F., Mohammadi, M., Najafpour, G. D., & Moghadamnia, A. A. (2017). Enzyme-assisted ionic liquid extraction of bioactive compound from turmeric (*Curcuma longa* L.): Isolation, purification and analysis of curcumin. *Industrial Crops and Products*, 95, 686–694. <https://doi.org/10.1016/j.indcrop.2016.11.037>
- Sahraee, S., Milani, J. M., Ghanbarzadeh, B., & Hamishehkar, H. (2017). Effect of corn oil on physical, thermal, and antifungal properties of gelatin-based nanocomposite films containing nano chitin. *Lebensmittel-Wissenschaft und -Technologie: Food Science and Technology*, 76, 33–39. <https://doi.org/10.1016/j.lwt.2016.10.028>
- Salaberria, A. M., Diaz, R. H., Andrés, M. A., Fernandes, S. C. M., & Labidi, J. (2017). The antifungal activity of functionalized chitin nanocrystals in poly (Lactid Acid) films. *Materials*, 10(5), 1–16. <https://doi.org/10.3390/ma10050546>
- Salaberria, A. M., Diaz, R. H., Labidi, J., & Fernandes, S. C. M. (2015a). Preparing valuable renewable nanocomposite films based exclusively on oceanic biomass - chitin nanofillers and chitosan. *Reactive and Functional Polymers*, 89, 31–39. <https://doi.org/10.1016/j.reactfunctpolym.2015.03.003>
- Salaberria, A. M., Diaz, R. H., Labidi, J., & Fernandes, S. C. M. (2015b). Role of chitin nanocrystals and nanofibers on physical, mechanical and functional properties in thermoplastic starch films. *Food Hydrocolloids*, 46, 93–102. <https://doi.org/10.1016/j.foodhyd.2014.12.016>
- Salaberria, A. M., Fernandes, S. C. M., Diaz, R. H., & Labidi, J. (2015). Processing of α -chitin nanofibers by dynamic high pressure homogenization: Characterization and antifungal activity against *A. Niger*. *Carbohydrate Polymers*, 116, 286–291. <https://doi.org/10.1016/j.carbpol.2014.04.047>
- Salaberria, A. M., Labidi, J., & Fernandes, S. C. M. (2015c). Different routes to turn chitin into stunning nano-objects. *European Polymer Journal*, 68, 503–515. <https://doi.org/10.1016/j.eurpolymj.2015.03.005>
- Salari, M., Sowti Khiabani, M., Rezaei Mokarram, R., Ghanbarzadeh, B., & Samadi Kafil, H. (2018). Development and evaluation of chitosan based active nanocomposite films containing bacterial cellulose nanocrystals and silver nanoparticles. *Food Hydrocolloids*, 84, 414–423. <https://doi.org/10.1016/j.foodhyd.2018.05.037>
- Sani, I. K., Pirsá, S., & Tağı, Ş. (2019). Preparation of chitosan/zinc oxide/Melissa officinalis essential oil nano-composite film and evaluation of physical, mechanical and antimicrobial properties by response surface method. *Polymer Testing*, 79. <https://doi.org/10.1016/j.polymertesting.2019.106004>
- Shen, Z., & Kamdem, D. P. (2015). Development and characterization of biodegradable chitosan films containing two essential oils. *International Journal of Biological Macromolecules*, 74, 289–296. <https://doi.org/10.1016/j.ijbiomac.2014.11.046>
- Sigurdson, G. T., Robbins, R. J., Collins, T. M., & Giusti, M. M. (2019). Molar absorptivities (ϵ) and spectral and colorimetric characteristics of purple sweet potato anthocyanins. *Food Chemistry*, 271, 497–504. <https://doi.org/10.1016/j.foodchem.2018.07.096>
- Silva Damasceno, E. T., Almeida, R. R., de Carvalho, S. Y. B., de Carvalho, G. S. G., Mano, V., Pereira, A. C., et al. (2018). Lippia origanoides Kunth. essential oil loaded in nanogel based on the chitosan and p-coumaric acid: Encapsulation efficiency and antioxidant activity. *Industrial Crops and Products*, 125(September), 85–94. <https://doi.org/10.1016/j.indcrop.2018.08.074>
- Silva-Pereira, M. C., Teixeira, J. A., Pereira-Júnior, V. A., & Stefani, R. (2015). Chitosan/corn starch blend films with extract from Brassica oleraceae (red cabbage) as a visual indicator of fish deterioration. *Lebensmittel-Wissenschaft & Technologie*, 61(1), 258–262. <https://doi.org/10.1016/j.lwt.2014.11.041>
- Souza, J. M., Caldas, A. L., Tohidi, S. D., Molina, J., Souto, A. P., Figueiro, R., et al. (2014). Original article Properties and controlled release of chitosan microencapsulated limonene oil. *Revista Brasileira de Farmacognosia*, 24(6), 691–698. <https://doi.org/10.1016/j.bjp.2014.11.007>
- Uranga, J., Etxabide, A., Guerrero, P., & de la Caba, K. (2018). Development of active fish gelatin films with anthocyanins by compression molding. *Food Hydrocolloids*, 84 (May), 313–320. <https://doi.org/10.1016/j.foodhyd.2018.06.018>
- Wiczowski, W., Szawara-Nowak, D., & Topolska, J. (2013). Red cabbage anthocyanins: Profile, isolation, identification, and antioxidant activity. *Food Research International*, 51(1), 303–309. <https://doi.org/10.1016/j.foodres.2012.12.015>
- Wu, C., Li, Y., Sun, J., Lu, Y., Tong, C., Wang, L., et al. (2020). Novel konjac glucomannan films with oxidized chitin nanocrystals immobilized red cabbage anthocyanins for intelligent food packaging. *Food Hydrocolloids*, 98, 105245. <https://doi.org/10.1016/j.foodhyd.2019.105245>
- Yong, H., & Liu, J. (2020). Recent advances in the preparation, physical and functional properties, and applications of anthocyanins-based active and intelligent packaging films. *Food Packaging and Shelf Life*, 26, 100550. <https://doi.org/10.1016/j.fpsl.2020.100550>
- Yong, H., Wang, X., Bai, R., Miao, Z., Zhang, X., & Liu, J. (2019). Development of antioxidant and intelligent pH-sensing packaging films by incorporating purple-fleshed sweet potato extract into chitosan matrix. *Food Hydrocolloids*, 90, 216–224. <https://doi.org/10.1016/j.foodhyd.2018.12.015>
- Yong, H., Wang, X., Zhang, X., Liu, Y., Qin, Y., & Liu, J. (2019a). Effects of anthocyanin-rich purple and black eggplant extracts on the physical, antioxidant and pH-sensitive properties of chitosan film. *Food Hydrocolloids*, 94, 93–104. <https://doi.org/10.1016/j.foodhyd.2019.03.012>
- Yun, D., Cai, H., Liu, Y., Xiao, L., Song, J., & Liu, J. (2019). Development of active and intelligent films based on cassava starch and Chinese bayberry (*Myrica rubra* Sieb. et Zucc.) anthocyanins. *RSC Advances*, 9(53), 30905–30916. <https://doi.org/10.1039/c9ra06628d>
- Zhai, X., Shi, J., Zou, X., Wang, S., Jiang, C., Zhang, J., et al. (2017). Novel colorimetric films based on starch/polyvinyl alcohol incorporated with rosele anthocyanins for fish freshness monitoring. *Food Hydrocolloids*, 69, 308–317. <https://doi.org/10.1016/j.foodhyd.2017.02.014>
- Zhang, X., Li, Y., Guo, M., Jin, T. Z., Arabi, S. A., He, Q., et al. (2021). Antimicrobial and UV blocking properties of composite chitosan films with curcumin grafted cellulose nanofiber. *Food Hydrocolloids*, 112, 106337. <https://doi.org/10.1016/j.foodhyd.2020.106337>
- Zhang, X., Liu, Y., Yong, H., Qin, Y., Liu, J., & Liu, J. (2019a). Development of multifunctional food packaging films based on chitosan, TiO₂ nanoparticles and anthocyanin-rich black plum peel extract. *Food Hydrocolloids*, 94, 80–92. <https://doi.org/10.1016/j.foodhyd.2019.03.009>
- Zhang, J., Zou, X., Zhai, X., Huang, X. W., Jiang, C., & Holmes, M. (2019). Preparation of an intelligent pH film based on biodegradable polymers and rosele anthocyanins for monitoring pork freshness. *Food Chemistry*, 272, 306–312. <https://doi.org/10.1016/j.foodchem.2018.08.041>
- Zhou, X., Yu, X., Xie, F., Fan, Y., Xu, X., Qi, J., et al. (2021). pH-responsive double-layer indicator films based on konjac glucomannan/camellia oil and carrageenan/anthocyanin/curcumin for monitoring meat freshness. *Food Hydrocolloids*, Article 106695. <https://doi.org/10.1016/j.foodhyd.2021.106695>
- Zhu, X., Chen, J., Hu, Y., Zhang, N., Fu, Y., & Chen, X. (2021). Tuning complexation of carboxymethyl cellulose/cationic chitosan to stabilize Pickering emulsion for curcumin encapsulation. *Food Hydrocolloids*, 110, Article 106135. <https://doi.org/10.1016/j.foodhyd.2020.106135>
- Zubillaga, V., Alonso-varona, A., Fernandes, S. C. M., Salaberria, A. M., & Palomares, T. (2020). Adipose-derived mesenchymal stem cell chondrospheroids cultured in hypoxia and a 3D porous chitosan/chitin nanocrystal scaffold as a platform for cartilage tissue engineering. *International Journal of Molecular Sciences*, 21(3), 1–17. <https://doi.org/10.3390/ijms21031004>
- Zubillaga, V., Salaberria, A. M., Palomares, T., Alonso-Varona, A., Kootala, S., Labidi, J., et al. (2018). Chitin nanofibers provide mechanical and topological cues to support growth of human adipose stem cells in chitosan matrices. *Biomacromolecules*, 19(7), 3000–3012. <https://doi.org/10.1021/acs.biomac.8b00570>